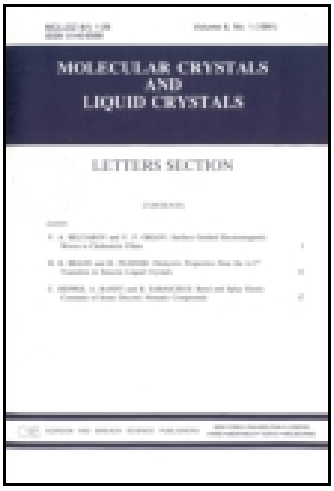

Molecular Crystals and Liquid Crystals
Publication details, including instructions for authors and subscription information:
http://www.tandfonline.com/loi/gmcl20

Soft Matter and Optical Vortices: A Good Match for New Science and Technology

L. Marrucci[ab]
[a] Dipartimento di Fisica, Università di Napoli "Federico II", Complesso di Monte S. Angelo, via Cintia, Napoli, Italy
[b] CNR-SPIN, Complesso di Monte S. Angelo, via Cintia, Napoli, Italy
Published online: 30 Sep 2014.

To cite this article: L. Marrucci (2014) Soft Matter and Optical Vortices: A Good Match for New Science and Technology, Molecular Crystals and Liquid Crystals, 595:1, 9-20, DOI: 10.1080/15421406.2014.917506

To link to this article: http://dx.doi.org/10.1080/15421406.2014.917506

Mol. Cryst. Liq. Cryst., Vol. 595: pp. 9–20, 2014

ISSN: 1542-1406 print/1563-5287 online
DOI: 10.1080/15421406.2014.917506

Taylor & Francis
Taylor & Francis Group

Soft Matter and Optical Vortices: A Good Match for New Science and Technology

L. MARRUCCI*

Dipartimento di Fisica, Università di Napoli "Federico II", Complesso di Monte S. Angelo, via Cintia, Napoli, Italy
CNR-SPIN, Complesso di Monte S. Angelo, via Cintia, Napoli, Italy

The interaction of soft materials with optical vortices can give rise to exciting new science and technology. In this paper, I will review a few recent examples of research based on such combination. In particular, I will consider the recently demonstrated applications of the liquid crystal "q-plates" to quantum communication without the need to align the reference frames of the communicating parties and to ultra-sensitive measurement of rotation angles, the latter by the new device concept dubbed "photonic gears". Moreover, I will discuss the observation of nanometric spiral-shaped structures generated by vortex light on the surface of azopolymers.

Keywords Liquid crystals; azopolymers; orbital angular momentum; optical vortex

I. Introduction

Soft materials, such as liquid crystals (LC) or polymers, often show particularly interesting optical properties. For example, liquid crystals are highly birefringent as some ordinary crystals, yet they can be easily patterned in microscopic structures and controlled by external fields, thanks to the softness of the molecular director and its sensitivity to boundaries [1]. These properties make liquid crystals the materials of choice for manufacturing Pancharatnam-Berry phase optical elements (PBOEs) for the visible domain [2–4], with the added advantage of allowing electric switching and tunability [5, 6]. In particular, q-plates are PBOEs designed to generate optical vortices or other azimuthally-structured modes of light [3–7], and have found a number of interesting classical and quantum photonic applications in the last few years [8–10]. On the other hand, soft materials in general may be particularly sensitive to light, giving rise to a number of nonlinear optical phenomena [11–14]. These phenomena, in turn, may reveal unexpected features when the irradiating light is spatially structured, e.g. with an optical vortex or more complex patterns. In particular, phenomena involving light absorption may be extremely efficient and eventually give rise to permanent changes in some materials [15–17].

In this paper, I will review three examples of the scientifically-fruitful interaction between vortex light and soft matter. After a short introduction in Section II on q-plates and orbital angular momentum, in Section III I will discuss the recent application of q-plates to the quantum communication without aligning the transmitting and receiving parties [18].

*Address correspondence to L. Marrucci, Dipartimento di Fisica, Università di Napoli "Federico II", Complesso di Monte S. Angelo, via Cintia, 80126, Napoli, Italy. Tel.:+39-081-676124; E-mail: lorenzo.marrucci@na.infn.it

This is based on using q-plates to generate states of light which are perfectly invariant under azimuthal rotations around the beam axis. The same concept can be also reversed, i.e., using q-plates to generate states of light which are extremely sensitive to rotations. This idea leads to the "polarization gears" photonic device and the corresponding super-resolving Malus' law [19], which will be discussed in Section IV. The polarization gears can be exploited to realize very sensitive contactless optical sensors of mechanical rotation of new design. Finally, in Section V, I will briefly illustrate the phenomenon of light-induced mass transport generated by vortex light in azopolymers and the ensuing theoretical analysis [20].

II. Q-Plates and Orbital Angular Momentum of Light

A q-plate is built as a planar LC cell having thickness and birefringence selected so as to induce a homogeneous birefringent phase retardation δ at the working wavelength λ, for light propagation perpendicular to the cell plane walls (z axis) [3, 4]. A q-plate is said to be *tuned* if $\delta = \pi$ (modulo 2π), and in the following we will assume that this condition is always fulfilled (either by proper temperature tuning or, more conveniently, by electric-field tuning [5, 6]). The LC nematic director $\mathbf{n}$ is assumed to be uniform in the z direction, but inhomogeneous in the xy plane of the cell, according to a prescribed pattern $\mathbf{n}(x,y) = \mathbf{n}(r,\phi)$, where r and ϕ are the polar coordinates in the xy plane. In particular, the q-plate pattern is specified by the following expression:

$$\alpha\,(r,\phi) = \alpha_0 + q\phi \tag{1}$$

where $\alpha(r,\phi)$ is the angle between the projection of the director $\mathbf{n}(x,y)$ on the xy plane and the x axis, α_0 is a constant angle specifying the director "initial" orientation on the axis x, and q is an integer or half-integer constant specifying the q-plate *topological charge*. Current q-plates are prepared by a non-contact photo-alignment technique, enabling the manufacture of electrically-tuned q-plates with arbitrary topological charge q [7]. A similar technique has been also used by other groups for preparing polymer-LC q-plates, although these devices do not include the electric tuning feature [21].

We are mainly interested in the action of the q-plate on optical fields that have a structure along the azimuthal coordinate. In particular, optical fields carrying *orbital angular momentum* (OAM) are characterized by a vortex phase factor $e^{im\phi}$, where m is an arbitrary integer [22]. For $m \neq 0$, this factor, together with the standard wave-propagation factor $e^{i(kz-\omega\,t)}$, defines a helical wavefront for the optical wave, with an optical vortex placed on the beam axis z (while for $m = 0$ we have a normal plane wave). It can be shown that this vortex factor is associated with an angular momentum oriented along z and given by $m\hbar$ per photon, where $\hbar$ is the reduced Planck constant, which comes *in addition* to the standard angular momentum $\pm\hbar$ per photon associated with circular polarization, commonly named as *spin angular momentum* (SAM) [22]. Optical fields carrying OAM form a set of eigenmodes for the azimuthal coordinate, so that fields having arbitrary azimuthal structures can be always decomposed in OAM eigenmodes.

Let us now assume that at the q-plate input face there is a circularly polarized wave having an arbitrary OAM with number m. In the paraxial approximation, its electric-field vector is

$$E_{in}\,(r,\varphi) = E_0\,(r) \begin{bmatrix} 1 \\ \pm i \\ 0 \end{bmatrix} e^{i(kz-\omega t)+im\varphi} \tag{2}$$

where $E_0\,(r)$ is an arbitrary radially-dependent amplitude and $\pm$ is $+$ for the left-circular case and $-$ for the right-circular one. At the q-plate output, we then obtain the following field [3, 23]:

$$E_{out}\,(r,\varphi) = E_0\,(r)\,e^{\pm i2\alpha_0 + i\chi}\begin{bmatrix}1\\ \mp i\\ 0\end{bmatrix} e^{i(kz-\omega t)+im'\varphi} \tag{3}$$

where

$$m' = m \pm 2q, \tag{4}$$

and χ denotes a constant global phase (unimportant for most purposes). This output field thus shows a reversed circular polarization, with respect to the input one, and a shifted OAM given by the integer m'.

It can be also useful to introduce a more synthetic "quantum-like" notation to describe the optical effect of a q-plate. The transformations induced by the q-plate on circularly polarized light carrying OAM can be then rewritten as follows:

$$\begin{aligned}\left|L,m\right\rangle &\xrightarrow{\text{q-plate}} \left|R,m+2q\right\rangle\\ \left|R,m\right\rangle &\xrightarrow{\text{q-plate}} \left|L,m-2q\right\rangle\end{aligned} \tag{5}$$

where the first symbol in the ket indicates the polarization state (L, for left-circular and R for right- circular) and the second is the OAM quantum number. This behavior is pictorially illustrated in Fig. 1. It should be noted that these transformations are also reversible, that is the q-plates can transform the right-hand side terms into the left-hand side ones as well. Most importantly, the q-plate is a coherent device that conserves linear combinations, so that an input light having an arbitrary (generally elliptical) polarization is transformed according to the following law:

$$\left(\alpha\left|L\right\rangle_p + \beta\left|R\right\rangle_p\right)\left|m\right\rangle_o = \alpha\left|L,m\right\rangle + \beta\left|R,m\right\rangle \xrightarrow{\text{q-plate}} \alpha\left|R,m+2q\right\rangle + \beta\left|L,m-2q\right\rangle \tag{6}$$

In the first expression on the left-hand-side of this equation we have used a notation separating the polarization degree of freedom (labeled with a subscript p) and the OAM one (labeled with a subscript o), so as to show more clearly that the input wave has a single well-defined elliptical polarization and a single OAM value. At the output, on the contrary, we obtain a non-separable optical state, in which polarization and OAM are "entangled", which corresponds to a space-variant polarization. Equation (6) is at the basis of many demonstrated quantum applications of the q-plate [24, 25].

We should emphasize that Eqs. (5) and (6) omit to describe the effect of the q-plate on the radial profile of the optical wave. This effect has been discussed in Refs. [26–28]. In many applications, this radial effect can be ignored, either because the radial profile factorizes and therefore is the same for all field components or because the propagation occurs on a sufficiently short distance that its effects remain negligible.

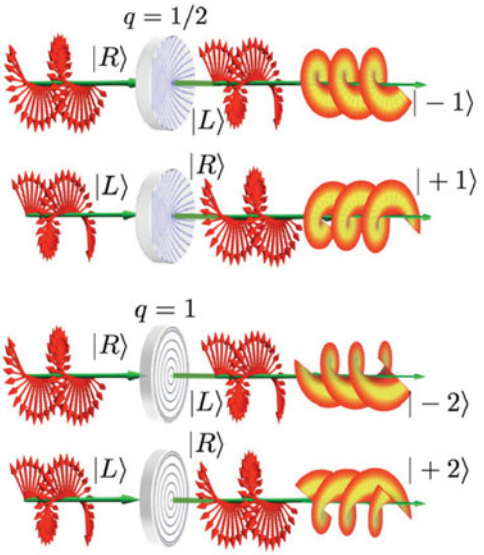

Figure 1. Effect of a tuned q-plate on input circularly polarized light having zero OAM. The upper two panels illustrate the case $q = 1/2$ for the two opposite circular polarizations. The lower two panels refer to the case $q = 1$. In all cases, the output polarization handedness is inverted and the output OAM acquires $\pm 2q\hbar$ of angular momentum, with the $\pm$ sign determined by the input polarization handedness [3]. Reproduced from Ref. [11], with permission from Taylor and Francis.

III. Rotation-invariant States of Light for Quantum Communication Without Alignment

Quantum communication is typically based on sending individual photons, each carrying a *qubit*, the elementary unit of quantum information. A qubit, as a classical bit, can have one of two values, which may be labelled 0 and 1. However, unlike a classical bit, a qubit can also reside in a quantum superposition of these two values, which in a quantum notation can be represented by the linear combination $\psi\rangle = \alpha|0\rangle + \beta|1\rangle$. The most common choice for implementing qubits with photons is the *polarization encoding*, which corresponds to associating two orthogonal polarization states to the 0 and 1 values (thus defining the so-called *logical basis*). For example, one may use two orthogonal linear polarizations, such as the horizontal (H) and vertical (V) ones, as defined in a given reference frame. An arbitrary polarization-encoded photonic qubit can then be represented as $|\psi\rangle = \alpha|H\rangle + \beta|V\rangle$, which corresponds also to an elliptical polarization state of the photon.

One problem of the described encoding system is its reliance on a shared reference frame for the transmitting and receiving parties. Indeed, if a common frame is not established, the exchanged qubits are affected by errors, arising from the unknown relative rotation of the two frames. One might naively think that this problem can be easily solved by using the circular polarization states L and R for the logical basis, because these states seem to be rotation-invariant. However, the circular polarization states are not truly rotation-invariant: under rotation, they are phase-shifted. The phase shift is opposite for L and R, so that an arbitrary qubit is altered by the rotation (it is not only a global phase shift) and the problem is not solved.

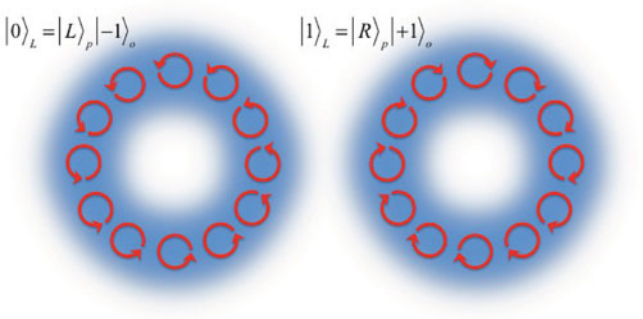

Figure 2. Schematic diagrams representing cross sections of the rotation-invariant photonic states used as logical basis to encode the quantum information in the alignment-free quantum communication protocol [18]. In particular, the left-side image represents the "logical zero" of the encoding and the right-side one the "logical one". The background "donuts" represent the intensity patterns of the Laguerre-Gauss modes carrying OAM = –1 (left) or +1 (right). Superimposed are the small circles representing the circular polarization states at each point, left-circular (labelled as "*L*") on the left side and right-circular (labelled as "*R*") on the right side. The optical phase is represented by the position of the arrow in the polarization circles and the helical structure of the wavefront emerges from the phase variation occurring when circling the beam center. These diagrams show that these photonic states are indeed fully rotation-invariant, including in the optical phase, and hence are suitable for encoding quantum information without the need to align the reference frames of the transmitting and receiving units. Reported are also the ket expressions of the corresponding quantum states.

The ideal solution would be to identify two orthogonal photonic states that are truly invariant under rotations, including their optical phase. Such states do indeed exist and are based on combining the polarization with the OAM. Indeed, the single quantity that controls the overall rotational dependence of a quantum state is the total angular momentum (TAM). A rotation invariance around the optical axis z is reflected into a vanishing TAM z-component J_z. As mentioned above, the polarization is associated to SAM, which is $S_z = \pm\hbar$ per photon, so it cannot vanish. However, the OAM brings in an additional term $L_z = m\hbar$, and setting $m = \pm 1$ one may obtain a TAM $J_z = S_z + L_z = 0$ and hence rotation-invariant states of light. The simplest choice is to consider the following two states:

$$|0\rangle_L = |L\rangle_p |-1\rangle_o , \quad |1\rangle_L = |R\rangle_p |+1\rangle_o \tag{7}$$

These states have opposite SAM and OAM and hence a vanishing TAM. They are also orthogonal to each other and hence can be taken as new logical basis for encoding qubits. The arbitrary photonic qubit will then be given by

$$|\psi\rangle = \alpha |0\rangle_L + \beta |1\rangle_L = \alpha |L\rangle_p |-1\rangle_o + \beta |R\rangle_p |+1\rangle_o \tag{8}$$

States of this form in general do not have a well defined uniform polarization, but a space-variant one, patterned in such a way that the states are globally rotation-invariant (including their phase) [29]. In particular, the two states of the logical basis are sketched in Fig. 2.

The main practical problem for doing quantum communication using these states is that of generating and reading them for single photons efficiently and with a high fidelity. Both these tasks can be simply accomplished by using q-plates with $q = 1/2$, as demonstrated in

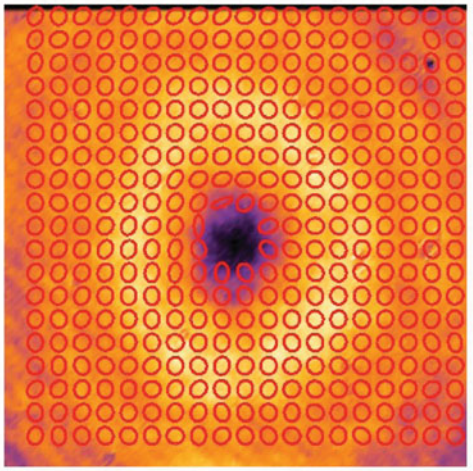

Figure 3. Intensity and polarization distributions in a cross section of a rotation-invariant photonic state generated by a q-plate with $q = 1/2$, as experimentally reconstructed from point-by- point polarimetry (in the near field immediately after the q-plate) [30]. The brightness at each point corresponds to the total light intensity while the small ellipses show the reconstructed polarization (the handedness is uniform and is omitted for simplicity).

Ref. [18]. Indeed, by inserting $q = 1/2$ and $m = 0$ in Eqs. (5), we obtain:

$$\begin{aligned} \left| L, 0\right\rangle &\overset{\text{q-plate}}{\underset{\longleftarrow}{\longrightarrow}} \left| R, +1\right\rangle = \left| 1\right\rangle_L \\ \left| R, 0\right\rangle &\overset{\text{q-plate}}{\underset{\longleftarrow}{\longrightarrow}} \left| L, -1\right\rangle = \left| 0\right\rangle_L \end{aligned} \tag{9}$$

in which we have also highlighted the fact that the induced transformations are reversible. Hence, a q-plate can transform an input polarization-encoded photonic qubit into a rotation-invariant qubit written using a hybrid polarization/OAM state and vice versa. This allows adapting the standard generation and detection methods used for polarization encoding to this rotation-invariant encoding, so as to obtain quantum communication that is insensitive to the relative orientation of the reference frames of the transmitting and receiving units [18]. Transformations (9) apply to single photon states but also to intense classical waves. Hence, they can be also tested in a classical regime: Fig. 3 shows the measured intensity and polarization profile of a rotation-invariant photonic state $\left|0\right\rangle_L = \left|L\right\rangle_{\mathrm{p}}\left|-1\right\rangle_o$ generated by a q-plate in a classical regime [30].

Although the described system was conceived to be independent of the relative orientation only for rotations around the beam axis linking the transmitting and receiving units, it is interesting to notice that tilts around different axes also do not affect the qubit transmission fidelity, and their only effect is to reduce the transmission quantum efficiency (or detection probability) [18]. This is a rather counterintuitive result, to be linked to the possibility of filtering out the perturbations induced in the spatial mode by exploiting the presence of polarization in the hybrid encoding.

IV. Photonic Polarization Gears

The main ingredients of the quantum communication without alignment described in the previous Section were the following two: (i) defining a pair of orthogonal photonic states that are truly rotation-invariant and (ii) developing a convenient method (based on a specific kind of q-plate) to convert ordinary polarization states into these rotation-invariant states and vice versa. The polarization gears is a photonic device that exploits the same pair of ingredients, but somehow "reversing" the first one [19]. In particular, in the place of rotation-invariant states, it exploits *highly rotation-sensitive photonic states*.

Just as rotation-invariant states of light are obtained by setting their TAM J_z to zero, highly rotation- sensitive states can be obtained by setting their TAM J_z to a very large value. Since the SAM is limited to $S_z = \pm\hbar$, this can only be done by using very large values of OAM, that is of $m\hbar$. For an OAM eigenstate, this rotation sensitivity is not easy to be detected, because it translates into a phase change only, arising from the vortex factor $e^{im\phi}$. However, one can change this into an easy-to- detect intensity modulation by considering superpositions of two OAM eigenstates with opposite values of m. These are modes of light exhibiting $2|m|$ bright "petals" when circling the beam axis once. Hence, by using for example a thin slit, one can detect the oscillations of the transmitted light and detect the rotation (see, e.g., Refs. [31, 32]).

However, in the photonic gear device the rotation is detected in a much simpler and more convenient way, that is by translating the photonic state back into a uniform-polarization one, by exploiting the q-plates, so that the rotation gets translated into a simple rotation of the polarization plane [19]. In other words, one arranges things so that a relative rotation of the reference frames of two objects by a given angle θ (that is, a mechanical rotation) gets translated into a rotation of the detected (uniform) polarization of light by an angle $(m + 1)\theta$, analogously to a mechanical gears device, which translates a given rotation of a mechanical element into an amplified (or reduced) rotation of another element. The *gears ratio* $m+1$ arises from the combined contributions of OAM (for the term m) and SAM (that adds $+1$). The photonic gears is based on the following layout: first, the light source is prepared in a given linear polarization state (say, H) and is then sent through a first q-plate (with fixed orientation) having a large value of the charge $q = m/2$ and then through a half-wave plate (HWP) to flip the circular polarization handedness. This leads to the following photonic transformations:

$$|H\rangle = \frac{1}{\sqrt{2}}(|L\rangle + |R\rangle) \xrightarrow{\text{q-plate}} \frac{1}{\sqrt{2}}(|R,m\rangle + |L,-m\rangle) \xrightarrow{HWP} \frac{1}{\sqrt{2}}(|L,m\rangle + |R,-m\rangle) \tag{10}$$

Then the light is sent to the rotated stage, where the rotation angle is θ. This frame rotation is equivalent to the following opposite-angle physical rotation of the photons:

$$\frac{1}{\sqrt{2}}(|L,m\rangle + |R,-m\rangle) \xrightarrow{\text{rotation by } \theta} \frac{1}{\sqrt{2}}\left(|L,m\rangle\, e^{-i(m+1)\theta} + |R,-m\rangle\, e^{+i(m+1)\theta}\right) \tag{11}$$

Then, the light is sent through another HWP and a second q-plate, with the same q as the first one, which are both fixed in the rotated stage, thus obtaining the following final transformations:

$$\frac{1}{\sqrt{2}}\left(|L,m\rangle\, e^{-i(m+1)\theta} + |R,-m\rangle\, e^{+i(m+1)\theta}\right) \xrightarrow{\text{HWP + q-plate}} \frac{1}{\sqrt{2}}\big(|L,0\rangle\, e^{-i(m+1)\theta} + |R,0\rangle\, e^{+i(m+1)\theta}\big) \tag{12}$$

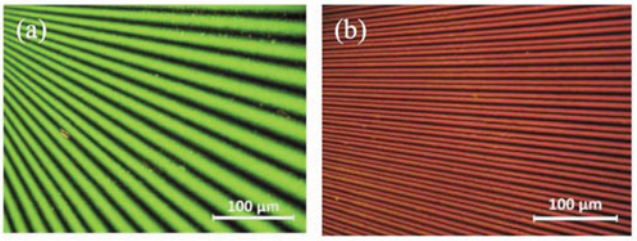

Figure 4. Images of q-plates with very high topological charge, as used in the photonic gears device [19]. (a) Microscope photo of a (non-central) sector of a q-plate with $q = 25$, imaged between crossed polarizers. Dark fringes correspond to regions with the molecular director parallel or perpendicular to the polarizer axes. (b) Microscope photo of a sector of a q-plate with $q = 150$, imaged between crossed polarizers. Photos by Sergei Slussarenko.

This final state has zero OAM and is therefore uniform in the azimuthal coordinate. Moreover, it is given by the balanced combination of two opposite circular polarization states, so it correspond to a linear polarization. However the phase factors appearing in the sum determine the orientation of the polarization plane, which forms an angle $(m + 1)\theta$ with the H direction. Hence, the outgoing polarization is again linear, but its oscillation plane is rotated with respect to the reference direction by an angle that is $m + 1 = 2q + 1$ times larger than the mechanical rotation (without the HWPs the scheme would still work, but the SAM would contribute in the wrong direction, and the enhancement factor would be m–1). After a linear polarizer fixed at the orientation H of the rotating frame, one then observes intensity modulations as a function of the rotation angle θ with an angular period that is reduced by the factor $m + 1$ with respect to the ordinary case of polarization only (without the q-plates). In other words, one observes what can be called a *super-resolving Malus' law*. This modulations, in turn, can be used to measure optically the mechanical rotation with greatly enhanced sensitivity.

In order to demonstrate this effect, q-plates with very large charge q, up to $q = 150$, were manufactured for the first time (see photos in Fig. 4). The photonic gears device and the resulting experimental super-resolving Malus' law for $q = 25$ ($m = 50$) are illustrated in Fig. 5.

V. Photoinduced Spiral Reliefs in Azopolymers

The last example I will review here is quite unrelated to the previous ones. In this case, the involved soft material is a thin film of azopolymer interacting with vortex light (that is, light carrying OAM). Azopolymers are fascinating for their sensitivity to light in the visible domain, which is mainly linked to the photo-isomerization processes induced in the azo groups, from the trans to the cis form and vice versa [13, 15]. In suitable materials, the transformation can be repeated back and forth many times, under constant irradiation. This may lead to large photoinduced rearrangements in the polymer, including a photoinduced molecular alignment effect and a photoinduced mass transport. The latter, in turn, leads to the appearance of surface relief patterns when the illuminating light is itself inhomogeneous (see, e.g., Ref. [33] for a recent review). For example, an interference grating can induce the appearance of a permanent relief grating on the polymer surface. A

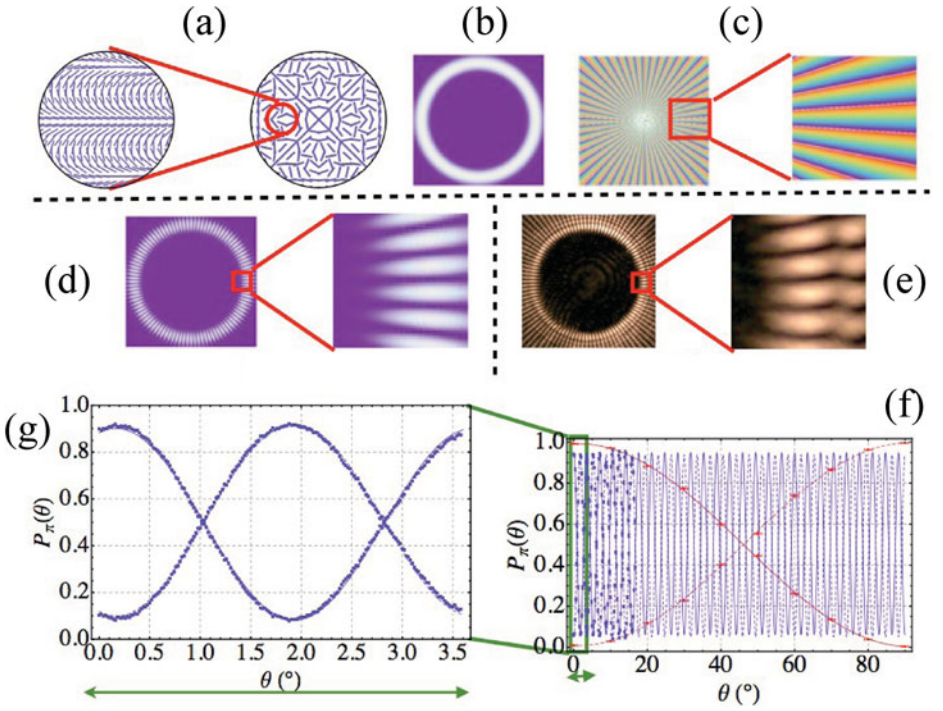

Figure 5. Illustration of the "photonic polarization gears" effect [19]. (a) Sketch of the liquid crystal molecular director alignment for a q-plate with $q = 25$, including a zoomed view of a smaller circular area. (b) Calculated donut-shaped light intensity distribution of a Laguerre-Gauss beam with azimuthal order (OAM) $m = 50$ as is generated by the q-plate for an input circular polarization, assuming the lowest-order radial profile. (c) Corresponding calculated phase distribution (in false colours), including a zoomed view of a smaller area. (d) Calculated intensity distribution obtained for an input linear polarization, that is a superposition of two opposite circular polarizations, showing 100 fringes in the azimuthal coordinate. (e) Corresponding measured intensity distribution. (f) Resulting measured (dots) and calculated (line) super-resolving Malus' law obtained for the corresponding photonic gears device. For comparison, the standard Malus' law is also shown. (g) Zoomed view of a section of the super-resolving Malus' law. Adapted from Ref. [19], with permission from Nature Publishing Group.

strongly focused single beam can induce instead localized surface reliefs on the micrometric or even sub-micrometric scale.

Although it is clear that the process is driven by the light absorption, the underlying physical mechanisms are still unclear and under investigation [33]. In particular, the mass transport and the resulting relief patterns are sensitive to light polarization (the transport tends to occur preferentially or even exclusively along the polarization direction). This surface patterning effect is not only interesting for fundamental reasons, but also because it is becoming a promising alternative technology for large-area patterning of photonic devices, replacing photoresists or other methods [33].

The recent observation that I am reviewing here is that, when the writing light is an optical vortex, the resulting relief pattern is shaped as a small spiral, with two arms (see Fig. 6 for an example) [20]. The spiral handedness is fixed by the optical vortex one. At first sight this might appear as not so surprising a result, because the spiral (helical)

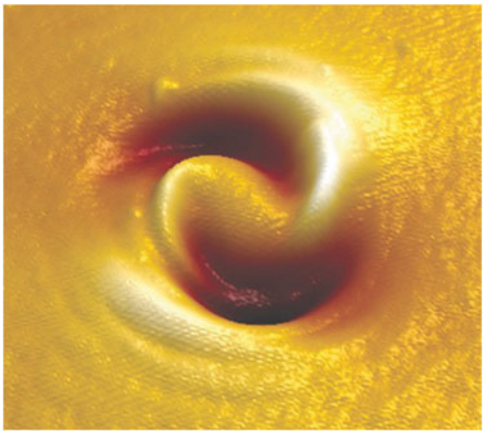

Figure 6. Atomic-force microscopy (AFM) image of the surface topography of an azopolymer after irradiation with a focused optical vortex with charge $m = 10$ [20]. The image side corresponds to an actual length of about 4 μm. The spiral relief height-to-depth full range corresponds to about 100 nm. Adapted from Ref. [20], with permission from Nature Publishing Group.

structure of light is translated into a spiral structure of the polymer. However, the result appears more striking if one considers that the intensity and polarization patterns of vortex light do not have any signature of the wavefront helical structure. In particular, they are identical for oppositely charged vortices. So, it seems that the polymer is somehow feeling

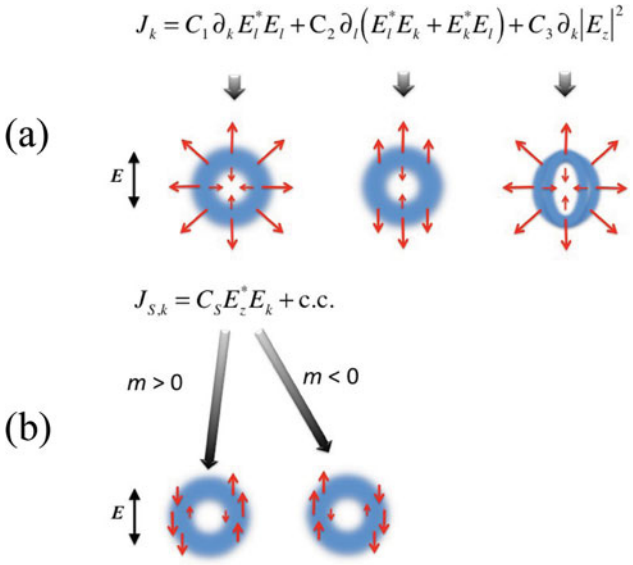

Figure 7. Sketch of the mass currents induced in the irradiated area of the azopolymer by different photoinduced terms that may be postulated by symmetry arguments, assuming that the illuminating light has a vortex structure, with a donut intensity profile. (a) The three standard gradient terms and the resulting currents, assuming a positive value of the coefficients and that the optical polarization is linear and oriented as indicated in figure. (b) Additional non-gradient term that may arise thanks to the surface-induced breaking of rotational symmetry and the ensuing currents, which depend on the vortex handedness, as given by the sign of the vortex charge m.

the wavefront structure, or the optical phase distribution, which is very surprising for an absorption-driven effect. Moreover, none of the models proposed in the past for this light-induced mass transport effect predicts this phase sensitivity and the appearance of the spiral structures.

The current interpretation of this puzzling effect has been linked to the vectorial sensitivity of the photoinduced mass transport effect and to the surface-induced breaking of rotational symmetry [20, 34]. Indeed, by combining these two elements, on symmetry grounds only one may propose a new mass current term (see Fig. 7) that is sensitive to the vortex handedness. This sensitivity, in turn, arises from the presence of an unusual interference term between the longitudinal field component (along the propagation direction z) and the transverse ones (in the transverse plane xy), which have comparable magnitude in a strongly focused beam. Indeed, the longitudinal and transverse field components of vortex beams have a different value of OAM, so that their interference retains memory of the OAM sign.

VI. Conclusions

In this paper, I have reviewed three examples of recent works in which the combination of soft matter and optical vortices, or light OAM, led to interesting new results in science and technology. Chances are good that this fruitful combination will continue producing interesting novel results in the near future. In particular, the liquid-crystal-based q-plate device has already shown a great potential for developing new classical and quantum photonic applications. In particular, the main potential advantage in the area of quantum information is that of using the higher dimensionality of OAM for encoding more qubits in a single photon [35], or equivalently to encode in each photon a so-called "qudit", i.e., a quantum state living in a d-dimensional space with $d > 2$ [9]. A recent result opens up also the possibility of translating photonic qudits into multiple photonic qubits and vice versa (although not yet in OAM), further enhancing the usefulness of this approach [36]. Classical results of q-plates are mainly being achieved in the area of singular optics [30, 37]. On another side, spatially-structured light, such as vortex light, can be useful to manufacture new complex structures in soft materials that are sensitive to light, and this approach in turn has the potential to become a convenient route to manufacturing novel photonic devices [38].

Acknowledgments

I acknowledge the financial support of the Future and Emerging Technologies (FET) programme within the Seventh Framework Programme for Research of the European Commission, under FET-Open grant number 255914, PHORBITECH.

References

[1] Blinov, L. M. & Chigrinov, V. G. (1996). *Electrooptic Effects in Liquid Crystal Materials*, Springer, New York.
[2] Bomzon, Z., Biener, G., Kleiner, V., & Hasman, E. (2002). *Opt. Lett.*, *27*, 1141.
[3] Marrucci, L., Manzo, C., & Paparo, D. (2006). *Phys. Rev. Lett.*, *96*, 163905.
[4] Marrucci, L., Manzo, C., & Paparo, D. (2006). *Appl. Phys. Lett.*, *88*, 221102.
[5] Karimi, E. *et al.* (2009). *Appl. Phys. Lett.*, *94*, 231124.
[6] Piccirillo, B. *et al.* (2010). *Appl. Phys. Lett.*, *97*, 241104.

[7] Slussarenko, S. *et al.* (2011). *Opt. Express*, *19*, 4085.
[8] Nagali, E. *et al.* (2009). *Nature Photon.*, *3*, 720–723.
[9] Nagali, E. *et al.* (2010). *Phys. Rev. Lett.*, *105*, 073602.
[10] Marrucci, L. *et al.* (2011). *J. Opt.*, *13*, 064001.
[11] Marrucci, L. *et al.* (2012). *Mol. Cryst. Liq. Cryst.*, *561*, 48.
[12] Khoo, I. C. (2009). *Phys. Rep.*, *471*, 221.
[13] Shibaev, V., Bobrovsky, A., & Boiko, N. (2003). *Prog. Polym. Science*, *28*, 729.
[14] Santamato, E., Maddalena, P., Marrucci, L., & Piccirillo, B. (1998). *Liq. Cryst.*, *25*, 357.
[15] Ikeda, T., & Tsutsumi, O. (1995). *Science*, *268*, 1873.
[16] Kreuzer, M., Marrucci, L., & Paparo, D. (2000). *J. Nonlinear Opt. Phys. Mater.*, *9*, 157.
[17] Kreuzer, M. *et al.* (2003). *Phys. Rev. E*, *68*, 011701.
[18] D'Ambrosio, V., Nagali, E., Walborn, S. P., Aolita, L., Slussarenko, S., Marrucci, L., & Sciarrino, F. (2012). *Nature Commun.*, *3*, 961.
[19] D'Ambrosio, V., Spagnolo, N., Del Re, L., Slussarenko, S., Li, Y., Kwek, L. C., Marrucci, L., Walborn, S. P., Aolita, L., & Sciarrino, F. (2013). *Nature Commun*, *4*, 2432.
[20] Ambrosio, A., L. Marrucci, F. Borbone, A. Roviello, & P. Maddalena (2012). *Nature Commun.*, *3*, 989.
[21] Nersisyan, S., Tabiryan, N., Steeves, D. M., & Kimball, B. R. (2009). *Opt. Express*, *17*, 11926.
[22] Franke-Arnold, S., Allen, L., & Padgett, M. J. (2008). *Laser & Photon. Rev.*, *2*, 299.
[23] Marrucci, L. (2008). *Mol. Cryst. Liq. Cryst.*, *488*, 148.
[24] Marrucci, L. (2007). *Proceedings of SPIE*, *6587*, 658708.
[25] Nagali, E. *et al.* (2009). *Phys. Rev. Lett.*, *103*, 013601.
[26] Karimi, E. *et al.* (2007) *Opt. Lett.*, *32*, 3053.
[27] Karimi, E., Piccirillo, B., Marrucci, L., & Santamato, E. (2009) *Opt. Lett.*, *34*, 1225.
[28] Nagali, E. *et al.* (2009). *Opt. Express*, *17*, 18745.
[29] Holleczek, A., Aiello, A., Gabriel, C., Marquardt, C., & Leuchs, G. (2011). *Opt. Express*, *19*, 9714.
[30] Cardano, F., Karimi, E., Slussarenko, S., Marrucci, L., de Lisio, C., & Santamato, E. (2012). *Appl. Opt.*, *51*, C1.
[31] Barnett, S. M., & Zambrini, R. (2006). *J. Mod. Opt.*, *53*, 613.
[32] Fickler, R. *et al.* (2012). *Science*, *338*, 640.
[33] Lee, S., Kang, H. S., & Park, J.-K. (2012). *Adv. Mater.*, *24*, 2069.
[34] Ambrosio, A., Maddalena, P., & Marrucci, L. (2013). *Phys. Rev. Lett.*, *110*, 146102.
[35] Molina-Terriza, G., Torres, J. P., & Torner, L. (2007). *Nature Phys.*, *3*, 305.
[36] Vitelli, C., Spagnolo, N., Aparo, L., Sciarrino, F., Santamato, E., & Marrucci, L. (2013). *Nature Photon.*, *7*, 521.
[37] Cardano, F., Karimi, E., Marrucci, L., de Lisio, C., & Santamato, E. (2013). *Opt. Express*, *21*, 8815.
[38] Moerland, R. J. *et al.* (2013). *Materials Horizons*, DOI: 10.1039/c3mh00008g.